NASA TM X- 70865

TIME-DEPENDENT 2.2 MeV AND
0.5 MeV LINES FROM SOLAR FLARES

H. T. WANG
R. RAMATY

MARCH 1975

GSFC ——— GODDARD SPACE FLIGHT CENTER ———
GREENBELT, MARYLAND

For information concerning availability
of this document contact:

Technical Information Division, Code 250
Goddard Space Flight Center
Greenbelt, Maryland 20771

(Telephone 301–982–4488)

Time-Dependent 2.2 MeV and 0.5 MeV
Lines from Solar Flares

H. T. Wang* and R. Ramaty
NASA-Goddard Space Flight Center
Greenbelt, Maryland   20771

Abstract

The time dependences of the 2.2 MeV and 0.51 MeV gamma-ray lines from solar flares are calculated and the results are compared with observations of the 1972, August 4 and 7 flares. The time lag between the nuclear reactions and the formation of these two lines are caused, respectively, by capture of the neutrons, and by deceleration of the positrons and decay of the radioactive nuclei. Our main results are: The calculation is consistent with the observed rise of the 2.2 MeV line on August 4, and it does not require different time dependences for the accelerated protons and electrons in the flare region. The above lags can explain the delayed gamma-ray emission observed on August 7. Positrons of energies greater than about 10 MeV could be detected in interplanetary space following large solar flares.

I. Introduction

Gamma-ray line emissions at 0.5, 2.2, 4.4 and 6.2 MeV and continuum emission up to about 7 MeV were detected from the 1972, August 4 flare (Chupp et al. 1973, 1975). Line emissions at 0.5 and 2.2 MeV were also detected from the 1972, August 7 flare, but only upper limits could be set on the 4.4 and 6.2 MeV lines and on the continuum from this flare. The lines at 0.5, 2.2, 4.4 and 6.2 MeV are believed to be due to positron annihilation, neutron capture, and deexcitations of nuclear levels in ^{12}C, and ^{13}N and ^{16}O, respectively; the continuum is most likely bremsstrahlung produced by relativistic electrons accelerated in the solar flare (Ramaty et al. 1975 and references therein).

The calculation of the time dependence of bremsstrahlung and gamma-ray lines from excited nuclei is in general straightforward because the gamma rays are emitted in a much shorter time than any of the characteristic times of the solar flare. However, because the time scales associated with positron annihilation and neutron capture in the solar atmosphere are comparable with the characteristic rise and decay times of flares, the calculation of line intensities at 0.51 and 2.2 MeV has to take into account in detail the production, slowing down, and annihilation or capture of positrons or neutrons. In the present paper, we calculate the time dependences of these two lines for the 1972, August 4 and August 7 flares.

The 37 GHz microwave data for these two flares are shown in Figure 1 (Croom and Harris 1973). On August 4 the gamma rays were observed from 0623 to 0633UT, a time interval of strong microwave emission. On August 7 the gamma rays were detected from 1538 to 1547UT. (The time intervals of

gamma-ray observations were determined by the position of the earth-orbiting satellites OSO-7 with respect to the sunlit side of Earth). The fact that during the gamma-ray observation time on August 7 the microwave emission was very small can explain the absence of the prompt continuum, and 4.4 and 6.2 MeV lines from this flare. The delayed emissions of the 2.2 and 0.51 MeV lines are probably caused by the finite capture time of the neutrons in the photosphere, and by the long half lives of some of the positrons emitters or the long slowing-down times of high-energy positrons from π^+ mesons.

II. Time - Dependent 2.2 MeV Emission

In a previous paper (Wang and Ramaty 1974), we have treated the propagation of neutrons in the solar atmosphere and the formation of the 2.2 MeV line by the reaction

$$n + p \rightarrow d + \gamma. \qquad\qquad (1)$$

(See also discussions in Ramaty et al. 1975). In this treatment a distribution of neutrons was released in the chromosphere or corona, and the path of each neutron after its release was followed by a computer Monte-Carlo simulation. The results are shown in Figure 2 and 3 for two assumptions on the photospheric ^3He abundance: $^3He/H = 0$ and $^3He/H = 5 \times 10^{-5}$. In these figures, $\phi(t-t_o, \theta, E_n)$ is the time-dependent 2.2 MeV flux at Earth resulting from a monoenergetic and isotropic neutron distribution released instantaneously at the Sun at the time t_o; E_n is the energy of the neutrons and θ is the gamma-ray emission angle between the earth-sun line and the vertical to the solar surface. In calculating the 2.2 MeV flux, an assumption on the photospheric ^3He abundance must be

made because the ^{3}He in the photosphere constitutes an important non-radiative sink for neutrons. Whereas neutron capture on H yields a 2.2 MeV photon according to reaction (1), capture on ^{3}He proceeds via the radiationless transition n + ^{3}He $\rightarrow$ ^{3}H + p, and hence produces no photons. Since the cross section for this reaction is larger than that for reaction (1) by a factor of about 1.7 x 10^4 (King and Goldstein 1949), if the photospheric ^{3}He/H ratio is about 5 x 10^{-5}, comparable to that observed in the solar wind (e.g. Geiss and Reeves 1972), nearly equal numbers of neutrons are captured on ^{3}He as on H.

The time-dependent 2.2 MeV flux from an arbitrary neutron source is given by

$$F_{2.2}(t,\theta) = \int_0^\infty dE_n \int_0^t dt_o \, Q_n(E_n,t_o) \, \phi(t-t_o, \theta, E_n), \qquad (2)$$

where $Q(E_n, t_o) \, dE_n$ is the number of neutrons produced per second at time t_o in the energy interval dE_n around E_n.

Neutron production in accelerated particle interactions with ambient material has been treated extensively (Ramaty et al. 1975 and references therein). In Figure 4 we show the neutron production spectrum evaluated by assuming that accelerated particles with power-law energy spectra interact with the ambient solar atmosphere in a thin-target model. This interaction model has been defined by Ramaty et al (1975) and is the only one used in the present paper. The elemental and isotopic abundances of both the ambient medium and the accelerated particles are those given by Cameron (1973). The parameter s is the spectral index of the accelerated particles, n is the density in the ambient medium, and N_p(>30 MeV) is the average number of protons with energies greater than 30 MeV in the interaction region.

If the energy spectrum of the accelerated particles does not change with time, then the time dependence of $Q_n(E_n,t)$ is the same as that of the instantaneous number of the accelerated nuclei. Direct information on this time dependence could be obtained by measuring the time profile of a prompt nuclear gamma-ray line such as the 4.43 MeV line from $^{12}C^{*4.43}$. Since no such data is available for any solar flare, we have used the intensity-time profile of highest frequency microwave data shown in Figure 1. Because microwave emission from solar flares is most likely due to gyrosynchrotron emission of energetic electrons (e.g. Holt and Ramaty 1969), by using the microwave data to determine the time dependence of the instantaneous number of accelerated protons, we assume that this time dependence is the same as that of the instantaneous number of accelerated electrons. In Section IV we discuss some of the consequences of different time dependences for these two particle populations.

We have fitted both the August 4 and 7 microwave time profile by the function

$$\rho(t) = \begin{cases} 2.4 \times 10^{-3} \ t + 3.45 \times 10^{-5} \ t^2 & 0 < t < 200 \\ 1.86 & 200 < t < 560 \\ 3.48 - 2.9 \times 10^{-3} \ t & 560 < t < 1100 \\ 0.29 \ \exp \ (- \ (t-1100)/186) & 1100 < t < 1400 \\ 0 & 1400 < t \end{cases} \qquad (3)$$

where t is in seconds, and t=0 is at $6^h22^m36^s$ UT on August 4, and at $15^h14^m40^s$ UT on August 7. As seen in Figure 1, this function gives a good fit to the microwave data at times greater than about 15^h24^m on August 7. Because the gamma-ray observations start about 14 minutes later, an exact

fit at earlier times is of no great importance. We have assumed that $\rho(t) = 0$ for $t > 1400$ sec. This means that neutrons were not produced after $15^h 38^m$ UT on August 7, and therefore all the observed 2.2 MeV photons from about $15^h 38^m$ to $15^h 47^m$ were due to neutrons produced before this time interval.

We have not attempted to fit the function $\rho(t)$ to the decaying part of the August 4 event because the gamma-ray observations stopped at 0633 UT before the onset of the decay. The fit of $\rho(t)$ to the earlier part of the microwave event on August 4 is quite good, as can again be seen from Figure 1.

In terms of the function $\rho(t)$, the instantaneous neutron production spectrum can be written as

$$Q_n(E_n, t) = n N_p(>30\text{MeV}) \, q_n(E_n) \, \rho(t), \qquad (4)$$

where the q_n's are shown in Figure 4. By substituting equation (4) into equation (2), and by using the results of Figures 2 and 3 and unpublished tables (Wang 1975) for $\phi(t-t_o, \theta, E_n)$, we have evaluated the time-dependent 2.2 MeV intensity at Earth, $F_{2.2}(t)$. Since the longitude and latitude of the August 4 and August 7 flares were E08, N14 and W36, N13, respectively, the angle θ in both cases is sufficiently small to allow the use of the curves with $\theta = 0$ in Figures 2 and 3.

The results are shown in Figure 5 for $s = 1.5$ and 3, and for two assumption on the photospheric ^{3}He abundance together with the time dependence of the neutron production rate, $\rho(t)$. The data points are for the August 4 flare, and we shall discuss them in Section IV. The delayed emission of 2.2 MeV gamma rays due to the finite capture time of the

neutrons can be seen both during the rise and the decay of the event.

In particular, for t>1400s, 2.2 MeV photons are still emitted even

though $\rho = 0$. The delay is longer for steeper proton spectra and less

photospheric ^{3}He. Such proton spectra produce more low-energy neutrons

which require longer capture times. These times are also longer if

there is no ^{3}He in the photosphere (Wang and Ramaty 1974).

III. Time-Dependent 0.51 MeV Emission

Line emission at 0.51 MeV results from positron annihilation.

The principal positron emitters, their decay rates, λ_i, and maximum

positron energies, E_{max}, are given in Table 1. The instantaneous

production rates of these emitters, q_i, have been calculated and are

shown in Figure 6 (Ramaty et al. 1975). These rates depend on the number

and spectrum of accelerated nuclei in the flare region, and on the density

of the ambient medium. As can be seen, for steep spectra (large values

of the spectral index s), positrons are produced mainly from radioactive

nuclei, while for flat spectra π^+ mesons are the principal sources of

positrons.

By assuming that the spectrum of accelerated nuclei does not change

with time, the production rate of positrons per unit energy interval

around E at time t is given by

$$Q_+(E,t) = nN_p(>30\text{MeV}) \sum_i \lambda_i q_i P_i(E) \int_{-\infty}^{t} \rho(t')\exp[-\lambda_i(t-t')]\,dt' , \qquad (5)$$

where $\rho(t)$ is given in equation (3) and $P_i(E)$ is the energy distribution

of positrons from the positron emitter i. For radioactive nuclei, $P_i(E)$

is the energy distribution of the positrons in the rest frame of the

positron emitters. This distribution gives a good approximation to the

positron energy spectrum in the frame of the Sun, because for accelerated particle spectra of interest in solar flares, positron emitters are produced with much smaller velocities than the positron velocities in the rest frame of the emitters. For pion decay, $P_i(E)$ has to be calculated from accelerator data for π^+ production and the kinematics of the $\pi^+ \to \mu^+ \to e^+$ decay (Ramaty 1974 and references therein).

We have performed these calculations and the resultant π^+ and e^+ spectra are shown in Figures 7 and 8, respectively. These spectra were calculated in the thin-target model with power-law energy spectra for the primary particles. Note that the integrals under the various curves in both Figures 7 and 8 are equal to the total positron production from π^+ decay shown in Figure 6.

Because of Doppler broadening, positrons which annihilate at high energies do not contribute to observable 0.51 MeV line emission. We therefore calculate the production rate of positrons of energies less than E_o, where E_o is an energy such that positrons annihilating below E_o produce a sufficiently narrow line which can be resolved from the continuum. This rate is given by

$$Q(t,<E_o) = \int_{E_o}^{\infty} [1-f_e(E)][1-p(E)] \ Q_+[E,t-t_{sd}(E)]dE, \qquad (6)$$

where f_e and p are the probabilities for escape and annihilation during deceleration, and t_{sd} is the slowing-down time from E to E_o. We assume that the escape probability is negligible below E_o. Based on the observed width of the 0.51 MeV line for the August 4 flare, the temperature in the annihilation region is less than about $10^7\,°K$ (Chupp et al. 1975), or E_o is less than $\sim$ 1 keV.

The functions $p(E)$ and $t_{sd}(E)$ can be calculated from the following equations:

$$p(E) = 1-\exp[-\int_{E_o}^{E}(\lambda_a/\dot{E}(E'))dE']$$ (7)

$$t_{sd}(E) = \int_{E_o}^{E}dE'/\dot{E}(E'),$$ (8)

where λ_a is the annihilation rate of positrons at energies greater than E_o (Heitler 1954), and $\dot{E}(E)$ is the positron energy loss rate in the ambient medium. We have evaluated equations (7) and (8), and the results are shown in Figure 9. In the calculation of $p(E)$ we have used the energy loss rate of electrons in neutral hydrogen (Berger and Seltzer 1964); in the calculation of $t_{sd}(E)$ we have added to $\dot{E}$ the energy loss due to synchroton radiation in a magnetic field B (e.g. Ramaty 1974). Since most of the annihilations and a major part of the slowing-down time take place at relativistic energies, the exact value of E_o in equations (7) and (8) is not important. The slowing down time, $t_{sd}(E)$, is a strong function of positron energy, and it depends on the density and magnetic field in the annihilation region. The probability for annihilation at relativistic energies also depends on these parameters, but because it is quite small (less than 0.2 for all energies of interest) we neglect its dependence on the magnetic field.

The positrons which have decelerated below E_o either free annihilate or form positronium; 25% of the positronium is formed in the singlet spin state and 75% in the triplet state. Positronium in the singlet state has a mean life of 1.2×10^{-10} s and annihilates into two 0.51 MeV gamma rays. Positronium in the triplet state has a mean life of 1.4×10^{-7} s, and if left undisturbed for a time period much longer than its mean life,

it annihilates into 3 gamma rays of energies less than 0.51 MeV.
Collisions with the ambient medium dissociate and quench triplet
positronium if the density of the medium is larger than about 10^{15} cm^{-3}
(Leventhal 1973). If these collisions and quenching can be ignored,
the production rate of 0.51 MeV photons, $Q_{2\gamma}$, is related to the
instantaneous number of positrons in the annihilation region, N_+, simply
by

$$Q_{2\gamma}(t) = (2\lambda_{fa} + 0.5\lambda_{pf})N_+(t), \qquad (9)$$

where N_+ satisfies the equation

$$\frac{dN_+}{dt} = -(\lambda_{fa} + \lambda_{pf})N_+ + Q(t, <E_o), \qquad (10)$$

and λ_{fa} and λ_{pf} are the free annihilation and positronium formation
rates, respectively. By combining the solution of equation (10) with
equation (9) we obtain

$$Q_{2\gamma}(t) = (2\lambda_{fa} + 0.5\lambda_{pf})\int_{-\infty}^{t} Q(t', <E_o)\exp[-(\lambda_{fa} + \lambda_{pf})(t-t')]dt'. \quad (11)$$

Then by combining equations (5), (6) and (11), and by performing one
time integral, we obtain that the time-dependent 0.51 MeV intensity
at Earth, $F_{0.51}(t) = Q_{2\gamma}(t)/(4\pi R^2)$, is given by

$$F_{0.51}(t) = \frac{N_{2\gamma}}{4\pi R^2} \, nN_p(>30 \text{ MeV})\sum_i q_i \int_0^{\infty} dE(1-f_e)(1-p)P_i(E) \, G(\tau), \qquad (12)$$

where $\tau = t - t_{sd}(E)$, $N_{2\gamma} = (2\lambda_{fa} + 0.5\lambda_{pf})/(\lambda_{fa} + \lambda_{pf})$, and

$$G(\tau) = \frac{\lambda_i(\lambda_{fa} + \lambda_{pf})}{\lambda_i - \lambda_{fa} - \lambda_{pf}} \int_{-\infty}^{\tau} dt' \, \rho(t')[\exp(-\lambda_i(\tau-t')) - \exp(-(\lambda_{fa} + \lambda_{pf})(\tau-t'))]. \quad (13)$$

The values of λ_{fa} and λ_{pf} depend on the temperature, density and
ionization state of the ambient medium. Above E_o, λ_{fa} and λ_a are essentially

identical and λ_{pf} is very small; below E_o, because of the Coulomb attraction between the electron and positron, $\lambda_{fa} > \lambda_a$. Values of λ_{fa} and λ_{pf} in a fully ionized medium were given by Ramaty et al. (1975) based on calculations of C. Werntz and C. Crannell (private communication). According to these calculations, $\lambda_{fa} + \lambda_{pf}$ increases with decreasing temperature.

As mentioned above, the temperature in the annihilation region is less than 10^7 °K, based on the upper limit on the width of the 0.51 MeV line for the August 4 flare (Chupp et al. 1975). Therefore, $\lambda_{fa} + \lambda_{pf} > 1.5 \times 10^{-14} n (s^{-1})$, the value of this parameter at 10^7 °K. This lower limit should be compared with the slowing-down times shown in Figure 9 and the radioactive decay times given in Table 1. Since for positrons from π^+ decay t_{sd}^{-1} is about $10^{-14} n (s^{-1})$, the slowing-down time of these positrons is longer than their free annihilation and positronium formation time. Therefore, the time dependence of the 0.51 MeV line from such positrons is determined mainly by slowing-down process. For positrons from radioactive nuclei, the decay rates, λ_i, are less than about $10^{-2} s^{-1}$ (see Table 1; the positron emitters ^{12}N and ^{19}Ne have a negligible contribution to the total positron production). Hence if the ambient density is larger than about $10^{12} cm^{-3}$, the time dependence of $F_{0.51}(t)$ for positrons from radioactive nuclei, is dominated by the decay rates of these nuclei. As discussed in Section IV, it is unlikely that the density is less than this value. Thus, the time dependence of the 0.51 MeV line is determined either by the slowing-down time of the positrons from π^+ decay, or by the mean lives of the radioactive nuclei, and it is quite insensitive to the free annihilation and positronium formation times. In our calculations we use $\lambda_{fa} + \lambda_{pf} = 3 \times 10^{-14} n (s^{-1})$ which corresponds to a completely ionized medium at 10^6 °K (See Figure 27 in Ramaty et al. 1975).

The values of λ_{fa} and λ_{pf}, together with the dissociation and quenching

processes of positronium, determine $N_{2\gamma}$, the number of 0.51 MeV photons per

positron of energy less than E_o. This parameter is between 0.5 and 2 but

its exact value is uncertian because of uncertainties in the various cross

sections. We allow it, therefore, to be a free parameter, along with f_e,

the escape probability of the positrons.

We have evaluated equation (12), and the results for f_e constant and

various densities and magnetic fields are shown in Figures 10 and 11,

for $s=3$ and $s=1.5$, respectively. The assumed time dependence of the nuclear

reactions rate, $\rho(t)$, is also shown in Figure 10.

For $s=3$ (Figure 10), most of the positrons result from radioactive

nuclei. Since the energies of these positrons are only about 1 MeV, the

effect of synchrotron losses is negligible, and therefore we consider the

$B=0$ case only. We see that if $n \gtrsim 10^{12} cm^{-3}$, the time dependence of $F_{0.51}(t)$

is almost independent of n. As discussed above, if $\rho(t)$ is given, then

$F_{0.51}$ for positrons from radioactive nuclei is determined

mainly by the mean lives of the positron emitters and not by the annihilation

or positronium formation processes. For $n = 10^{11} cm^{-3}$, however, the time

dependence of $F_{0.51}$ is determined both by $\lambda_{fa} + \lambda_{pf}$ which is density and

temperature dependent, and by the decay rates of the long-lived radioisotopes

^{11}C and ^{13}N.

For $s=1.5$ (Figure 11) a major part of the positrons are from π^+ decay

and have energies where the effect of the synchrotron losses is important.

In this case we have used two values of B: $B=0$ and $B=5\times10^{-4}n^{\frac{1}{2}}$ (gauss). For

the curves in Figure 11, only the slowing-down time of positrons from pions

and the mean lives of ^{11}C and ^{13}N have an effect on the time dependence of

$F_{0.51}(t)$. For $n=10^{14} cm^{-3}$, the slowing-down time is so short that for $t<1400$ s

$F_{0.51}(t)$ has the same time dependence as $\rho(t)$; for later times,

the positrons are mainly from ^{11}C and ^{13}N. For $n=10^{11}$ and 10^{12} cm^{-3},

the slowing-down times are longer and hence $F_{0.51}(t)$ is delayed with

respect to $\rho(t)$. For $t > 1400$ sec, at these densities, $F_{0.51}(t)$ is due

to long slowing-down times of positrons from π^+ decays.

IV. Comparison with Observations

The data points in Figure 5 are the measured 2.2 MeV flux on

August 4, normalized to the calculations. As can be seen, the calculated

rise of the 2.2 MeV line fits the data very well, indicating that our

calculations on neutron propagation and 2.2 MeV line formation are in

general valid. In order to determine $nN_p(>30 \text{ MeV})$ for the flare of

August 4, we calculate the average of $F_{2.2}(t)$ over the gamma-ray observation

time, and compare it with the measured average 2.2 MeV flux of 0.28

photons $cm^{-2}s^{-1}$ (Chupp et al. 1975). We obtain $nN_p(>30 \text{ MeV}) = 4.5 \times 10^{43}$

cm^{-3} for $^3He/H = 5 \times 10^{-5}$ and $nN_p(>30 \text{ MeV}) = 3.2 \times 10^{43} cm^{-3}$ for $^3He/H = 0$,

essentially independent of spectral index for $1.5 < s < 3$. These values are

almost the same as given by Ramaty et al. (1975) who did not take into

account the time dependences of the gamma-ray fluxes.

In order to determine $nN_p(>30 \text{ MeV})$ for the August 7 flare, we have

calculated the average of $F_{2.2}(t)$ over the gamma-ray observation time

for this flare as shown in Figure 5. By comparing these averages with

the observed flux of 0.069 photons $cm^{-2}s^{-1}$ (Chupp et al. 1975) we obtain

values of $nN_p(>30MeV)$ as shown in Table 2. (The values for $s=2$ were

obtained from calculations which are not plotted in Figure 5). The

values of nN_p (>30 MeV) shown in this table are larger than those obtained

for the August 4 flare by about one order of magnitude. This means that

during the peak of the August 7 flare, in addition to all the lines observed

on August 4, other weaker lines (Table 3 in Ramaty et al. 1975) could have

been observed if OSO-7 had not been behind the Earth during the main gamma-

ray event. However, we note that the deduction of nN_p on August 7 is

somewhat uncertain because the gamma rays were observed very late in the

event. For example, the decay of the accelerated protons which produce the

gamma rays could be slower than the decay of the accelerated electrons which

produce the microwaves. In this case, neutrons would still be produced

during the gamma-ray observation period, and hence we would deduce smaller

values of nN_p for the August 7 event than shown in Table 2.

We have compared the time-dependent 0.51 MeV data for the August 4

flare (Chupp et al. 1975) with our calculations. Even though the uncertain-

ties in these data are quite large, they are indicative of a rapid rise

(<100 seconds) in the intensity of this line. From the analysis of Ramaty

et al. (1975) it follows that for the August 4 flare a major part of the

positrons were produced from π^+ decay (based on the spectral index $s \leqslant 2$

of the accelerated particles deduced from the ratio of the 4.4 MeV to the

2.2 MeV lines). Then using the results of Figure 9, we find that in order

to slow down the positrons from pion decay, the density and magnetic field

in the annihilation region have to be larger than about $10^{12} cm^{-3}$ and 500

gauss, respectively. However, a lower magnetic field is also possible if

the density is larger than about $5 \times 10^{12} cm^{-3}$.

We next compare our calculations with data for the average 0.51 MeV

and 2.2 MeV flux over the interval of gamma-ray observations on August 4.

The ratios for these calculated averages are shown in Table 3 for $n=10^{12} cm^{-3}$,

$B=500$ gauss, $(1-f_e)N_{2\gamma} = 1$, and two choices of the photospheric ^{3}He

abundances. Also shown in this table is the measured ratio of 0.23 ± 0.08.

For the spectral index $s\sim2$ discussed above, $(1-f_e)N_{2\gamma}$ is less than

about 0.3. Since the lowest value of $N_{2\gamma}$ is 0.5, we conclude that some

of the positrons escape from the Sun before they annihilate. We shall

discuss the consequences of this result below.

We proceed now to compare our calculations with the 0.51 MeV obser-

vation on August 7. According Chupp et al. (1975) and Forest (private

communication 1975) the observed average 0.51 MeV flux from 1538-1547 UT

was $(3 \pm 1.5) \times 10^{-2}$ photons/cm^2. The data point in Figures 10 and 11 were

obtained by multiplying this flux with $4\pi R^2/(nN_p(>30$ MeV$))$, where the various

values of $nN_p(>30$ MeV$)$ are given in Table 2. For $s=3$ (Figure 10) the data

is below the calculations by a factor of at least 4, which implies that

$(1-f_e)N_{2\gamma}$ is less than about 0.25. For $s=1.5$ (Figure 11), $(1-f_e)N_{2\gamma}$ can be

as large as 0.5 if the ambient density in the annihilation region is larger

than about $10^{13} cm^{-3}$, but if the ambient density is $10^{12} cm^{-3}$ and $B=500$ gauss,

$(1-f_e)N_{2\gamma}$ has to be less than ~0.2. In general, the largest values of

$(1-f_e)N_{2\gamma}$ are obtained when the photospheric ^{3}He abundance is small and the

ambient density in the annihilation region is large. The former decreases

the number of protons required to produce the 2.2 MeV flux and hence also

predicts a lower 0.51 MeV intensity. The latter causes more rapid annihilation

of positrons and hence leads to a smaller delayed 0.51 MeV emission. But even

for the largest values of $(1-f_e)N_{2\gamma}$, both for the August 4 and August 7 flares

the conclusion seems to be that a significant fraction of the positrons escape from the Sun.

We proceed, therefore, to estimate the ratio of the number of positrons of energies greater than E to the number of protons of energies greater than E that escape from a solar flare. The total number of positrons of energies greater than E produced in the flare is given by $nN_p(>30 \text{ MeV}) \sum_i q_i P_i(>E) \int \rho(t)dt$, and a fraction f_e of these positrons escape. To obtain an estimate of the number of protons released from the flare, information obtained from the gamma rays in the thin-target model can be combined with data on the path length traversed by the nuclei before their escape from the interaction region. Such information is obtained from studies of deuteron and helium-3 abundances in accelerated nuclei from flares. The ^{2}H and ^{3}He observations from the 1972, August events (Webber et al. 1975), when compared with calculations of the production of these isotopes in nuclear reactions (Ramaty and Kozlovsky 1974) imply that the amount of matter traversed by relativistic particles is about 1.5 g cm^{-2}. This means that the product nt_1 is about 3×10^{13} cm^{-3}s, where t_1 is the interaction time of the particles at the Sun. If t_1 is also interpreted as the escape time of the particles from the interaction region, then the protons were released into the interplanetary medium at an average rate $N_p(>30 \text{ MeV})/t_1$, and the total number released is $[N_p(>30 \text{ MeV})/t_1]\int \rho(t)dt$. Therefore, the positron-to-proton ratio for the escaping particles is

$$(\frac{e^+}{p})(>E) = f_e[\sum_i q_i P_i(>E)]nt_1 (E/30 \text{ MeV})^{s-1}. \tag{14}$$

We have evaluated this equation for several values of s, nt_1 given above, q_i given in Figure 6, and $P_i(E)$ given in Figure 8. The results are shown

in Figure 12. All the positrons in this figure are from π^+ decay. Radio-active nuclei can contribute to the interplanetary positron flux only below about 2 MeV. For s = 1.5, the contribution from π^+ decay is still dominant at these energies. For steeper spectra, e^+/p is very small below 2 MeV. In addition, if nt_1 is $\sim 3 \times 10^{13}$ cm^{-3} s, positrons from radioactive nuclei, having energies less than ~ 2 MeV, will not escape from the flare region.

As can be seen, the positron-to-proton ratio peaks at about 30 to 60 MeV, and its value is about 10^{-3} f_e (for s≤2). Accoding to Kohl et al. (1973), the peak flux of protons of energies greater than 30 MeV following the August 7 flare was about 300 protons/(s cm^{2}sr). Using the above e^+/p ratio, we find that the peak positron flux following the August 7 flare was $\sim 0.3f_e$ positrons/ (s cm^{2}sr). This flux is larger than the galactic positron flux above 30 MeV by about a factor of $10^3 f_e$ and could have been observable with proper satellite-borne instrumentation.

V. Summary and Conclusions

We have evaluated time-dependent 2.2 MeV and 0.51 MeV line intensities for the 1972, August 4 and August 7 flares. The calculations were made by assuming that the instantaneous number of accelerated protons in the inter-action region has the same time dependence as the instantaneous number of accelerated electrons which produce observable microwave emission. The pro-duction rates of neutrons and positron emitters have the same time dependences as the instantaneous proton number. The time dependence of the 2.2 MeV line was then determined by using the results of a Monte-Carlo simulation of neutron propagation and 2.2 MeV photon production in the photosphere. For the 1972, August 4 flare, the observed rise of the 2.2 MeV line is in very good agreement with our calculations, an agreement which supports the assump-

tion that the instantaneous accelerated proton and electron numbers could have similar time dependences. The delayed 2.2 MeV emission observed for the 1972, August 7 flare could be due to the finite capture time of the neutrons in the photosphere. This interpretation implies that the prompt gamma-ray emissions on August 7, even though not observed because of the occultation of the satellite, were larger by about an order of magnitude than those on August 4. Alternatively, some of the delayed 2.2 MeV emission could have been produced by protons which were trapped in the interaction region for longer times than the electrons, and continued to produce neutrons even though the microwave flux was observed to be very low.

The time dependence of the 0.51 MeV line was determined by taking into account the slowing-down time of positrons from π^+ decay, the mean lives of the β^+-emitting nuclei, and the annihilation and positronium formation times of positrons with the ambient medium. The latter time, however, is always shorter than the slowing-down times of positrons from π^+ decay, and it is also shorter than the shortest mean life of the important radioactive nuclei if the ambient density is larger than about $10^{12} \, cm^{-3}$. Since the density in the annihilation region appears to be of at least this value, the time dependence of the 0.51 MeV line is determined mainly by the slowing-down process from high energies (~ 50 MeV) and the decay of the β^+ emitters.

The relatively large delayed 0.51 MeV emission on August 7, 1972 is most likely due to the long half lives of ^{11}C and ^{13}N, or the long slowing-down times of the positrons. These two effects predict different time dependences which could be distinguished by future observations.

The comparison of the observed intensities of the 2.2 and 0.5 MeV lines with the calculations seems to imply that a fraction of the positrons escape from the Sun. These positrons are most likely from π^+ decay, because the stoppin

range of such positrons is longer than the mean amount of matter
($\sim$1.5g cm^{-2}) traversed by relativistic particles in the 1972, August
flares as deduced from ^{3}He observations in accelerated particle fluxes.
We find that the ratio of positrons-to-protons above 30 MeV in these flares
could have been about 5x10^{-4}, and the absolute positron flux was larger
than the integral galactic flux at the same energy by a factor of about 10^3.

In summary, time-dependent 2.2 MeV and 0.51 MeV line emissions from
solar flares present very interesting and involved time dependences which
reflect not only the histories of the charged particles but also the physical
conditions of the gamma ray producing regions. These conditions could be
best studied by simultaneously observing a prompt gamma-ray line such as
the line at 4.43 from ^{12}C and the delayed 2.2 MeV and 0.51 MeV lines. The
former would unambiguously determine the time history of the accelerated
nuclei, while the latter would provide valuable information on the physics
of neutrons and positrons in solar flares, and on the physical conditions
of the gamma ray producing regions.

References

Berger, M. J. and Seltzer, S. M. 1964, Tables of Energy Losses and

Ranges of Electrons and Positrons, NASA SP-3012 (National Aeronautics

and Space Administration, Washington, D.C.).

Chupp, E. L., Forrest, D. J., Higbie, P. R., Suri, A. N., Tsai, C., and

Dunphy, P. O. 1973, Nature 241, 333.

Chupp, E. L., Forrest, D. J., and Suri, A. N. 1975, Proc. of IAU-COSPAR

Symposium No. 68, Solar γ, x and EUV Radiations, edited by S. Kane,

in press.

Cameron, A. G. W. 1973, Space Science Review 15, 121.

Croom, D. L. and Harris, L. D. J. 1973, World Data Center Rept. UAG-28

part I, Collected Data on August 1972 Solar Terrestrial Events, edited

by H. E. Coffey, p. 210.

Geiss, J. and Reeves, H. 1972, Astron. Astrophys. 18, 126.

Heitler, W. 1954, Quantum Theory of Radiation, Oxford University Press, London.

Holt, S. S. and Ramaty, R. 1969, Solar Physics, 8, 119.

King, L. D. P. and Goldstein, L. 1949, Phys. Rev. 75, 1302.

Kohl, J. W., Bostrom, C. O., and Williams, D. J. 1973, World Data Center

Rept. UAG-28 part II, Collected Data Reports on August 1972 Solar

Terrestrial Events, H. E. Coffey, editor, p. 330.

Leventhal, M. 1973, Ap. J.. Letters, 183, L197.

Ramaty, R. and Kozlovsky, B. 1974, Ap. J. 193, 729.

Ramaty, R. 1974, High Energy Particles and Quanta in Astrophysics, MIT

Press, F. B. McDonald and C. E. Fichtel, editors, p. 122.

Ramaty, R., Kozlovsky, B., Lingenfelter, R. E. 1975, Space Science Reviews,

in press.

Wang, H. T. 1975, Doctoral dissertation, University of Maryland.

Wang, H. T. and Ramaty, R. 1974, Solar Physics, 36, 129.

Webber, W. R., Roelof, E. C., McDonald, F. B., Teegarden, B. J. and
Trainor, J. H. 1975, Ap. J. (to be published).

Table 1

Principal Positron Emitters

Positron Emitter	λ_i (s^{-1})	Maximum Positron Energy (MeV)
μ^+	4.6×10^5	53
^{12}N	6.3×10^1	16.4
^{19}Ne	4×10^{-2}	2.2
^{14}O	9.8×10^{-3}	1.8 (99.4%) 4.1 (0.6 %)
^{15}O	5.6×10^{-3}	1.74
^{13}N	1.2×10^{-3}	1.19
^{11}C	5.6×10^{-4}	0.92

Table 2 Deduced Values of $nN_p(>30$ MeV$)$ for the August 7 Flare in cm^{-3}

	s=1.5	s=2	s=3
^{3}He/H = 0	3.3×10^{44}	2.9×10^{44}	1.8×10^{44}
^{3}He/H = 5×10^{-5}	7.4×10^{44}	6.3×10^{44}	3.6×10^{44}

.

Table 3 Deduced Ratios, $\overline{F}_{0.51}/\overline{F}_{2.2}$, for the August 7 Flare

$n = 10^{12}\,cm^{-3}$, B = 500 gauss, $N_{2\gamma}(1-f_e) = 1$

	s=1.5	s=2	s=3
^{3}He/H = 0	3.5	0.73	0.24
^{3}He/H = 5×10^{-5}	5	1.15	0.38

$(\overline{F}_{0.51}/\overline{F}_{2.2})_{observed} = 0.23 \pm 0.08$

Figure Captions

Figure 1 Time dependences for the 1972, August 4 and 7 flares. Solid line – the 37 GHz microwave emission (Croom and Harris 1973). Dashed line – assumed time dependence of the nuclear reaction rates. Time intervals of gamma-ray observation determined by the position of OSO-7 are also shown.

Figure 2 Time profiles of the 2.2 MeV line intensity at Earth multiplied by $4\pi R^2$, where R = 1 AU, produced by instantaneously released monoenergetic neutrons at time t_o. The parameter θ is the angle between the Earth–Sun line and the heliocentric radial direction through the flare. The ratio ^{3}He/H is the photospheric helium 3 abundance, and E_n is the energy of the neutrons.

Figure 3 Same as Figure 2

Figure 4 Neutron production spectra in the thin-target model. n is the density of the ambient medium, N_p(>30 MeV) is the number of protons of energies greater than 30 MeV, and s is the index of the assumed power-law energy spectrum.

Figure 5 Time dependence of the 2.2 MeV line for various spectral indexes s and photospheric ^{3}He abundances. The function $\rho(t)$ is the assumed time dependence of the rate of nuclear reactions. The data points are the measured 2.2 MeV flux on August 4, 1972, normalized to the calculations.

Figure 6 Production rate of positron emitters as a function of the spectral index s in the thin-target model.

Figure 7   Production spectra of π^+ mesons for various spectral indexes

s. E_π is the kinetic energy of the pion, and $\gamma_\pi = 1 + E_\pi/(m_\pi c^2)$.

Figure 8   Production spectra of positrons for various spectral indexes s.

$\gamma_e = 1 + E_e/(m_e c^2)$, where E_e is the electron kinetic energy.

Figure 9   Probability for positron annihilation in flight, p(E), and the

slowing-down time of a positron of energy E, $t_{sd}(E)$. B is the

magnetic field in gauss, and n is the density of the ambient

medium in cm^{-3}.

Figure 10   Time dependence of the 0.51 MeV line for s=3 for various ambient

densities n and B=0. $\rho(t)$ is the time dependence of the rate of

reactions. The data points are the observed average 0.51 MeV

flux for the 1972 August 7 flare, multiplied by $4\pi R^2/nN_p$, where

nN_p, for the two choices of $^3He/H$, is given in Table 2. f_e is

the escape probability of the positrons, and $N_{2\gamma}$ is the number

of 0.51 MeV photon obtained per positron when positronium

formation is taken into account.

Figure 11   Time dependence of the 0.51 MeV line for s=1.5 and for various

ambient densities and magnetic fields. $\rho(t)$ is the time dependence

of the rate of nuclear reactions. The data points are the

observed average 0.51 MeV flux for the 1972 August 7 flare,

multiplied by $4\pi R^2/nN_p$, where nN_p, for the two choices of $^3He/H$,

is given in Table 2. f_e is the escape probability of the positrons,

and $N_{2\gamma}$ is the number of 0.51 MV photon obtained per positron

when positronium formation is taken into account.

Figure 12   The integral positron-to-proton ratio for particles escaping from

the flare region. f_e is the escape probability of the positrons.

$P(t)$

4 AUG 1972

37 GHz

U T

6^{h}20^m 30^m 40^m 50^m

GAMMA RAY
OBSERVATIONS

$P(t)$

7 AUG 1972

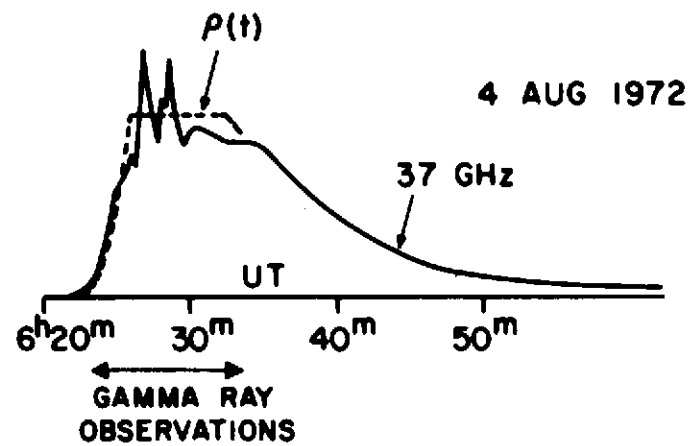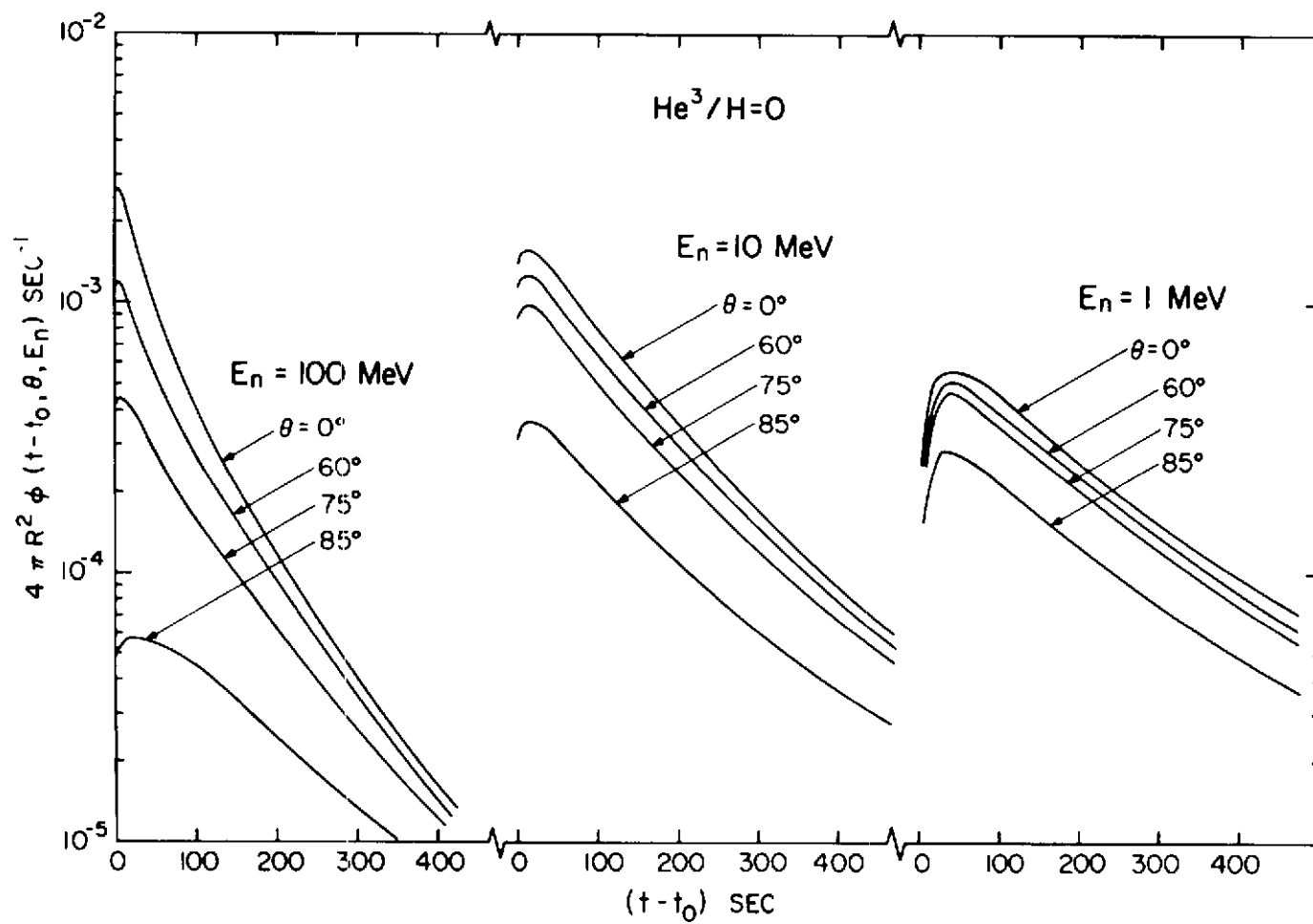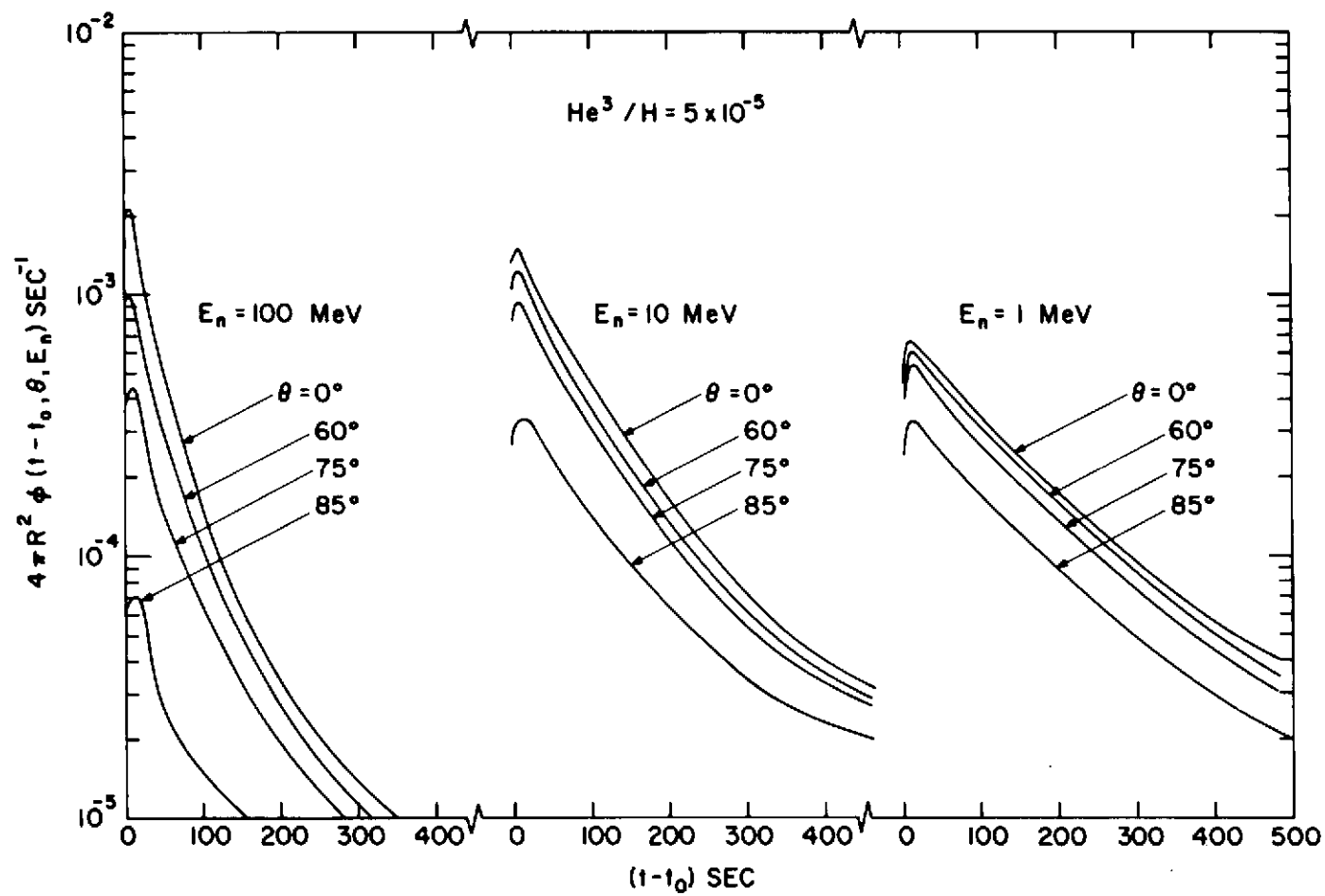37GH$_z$

U T

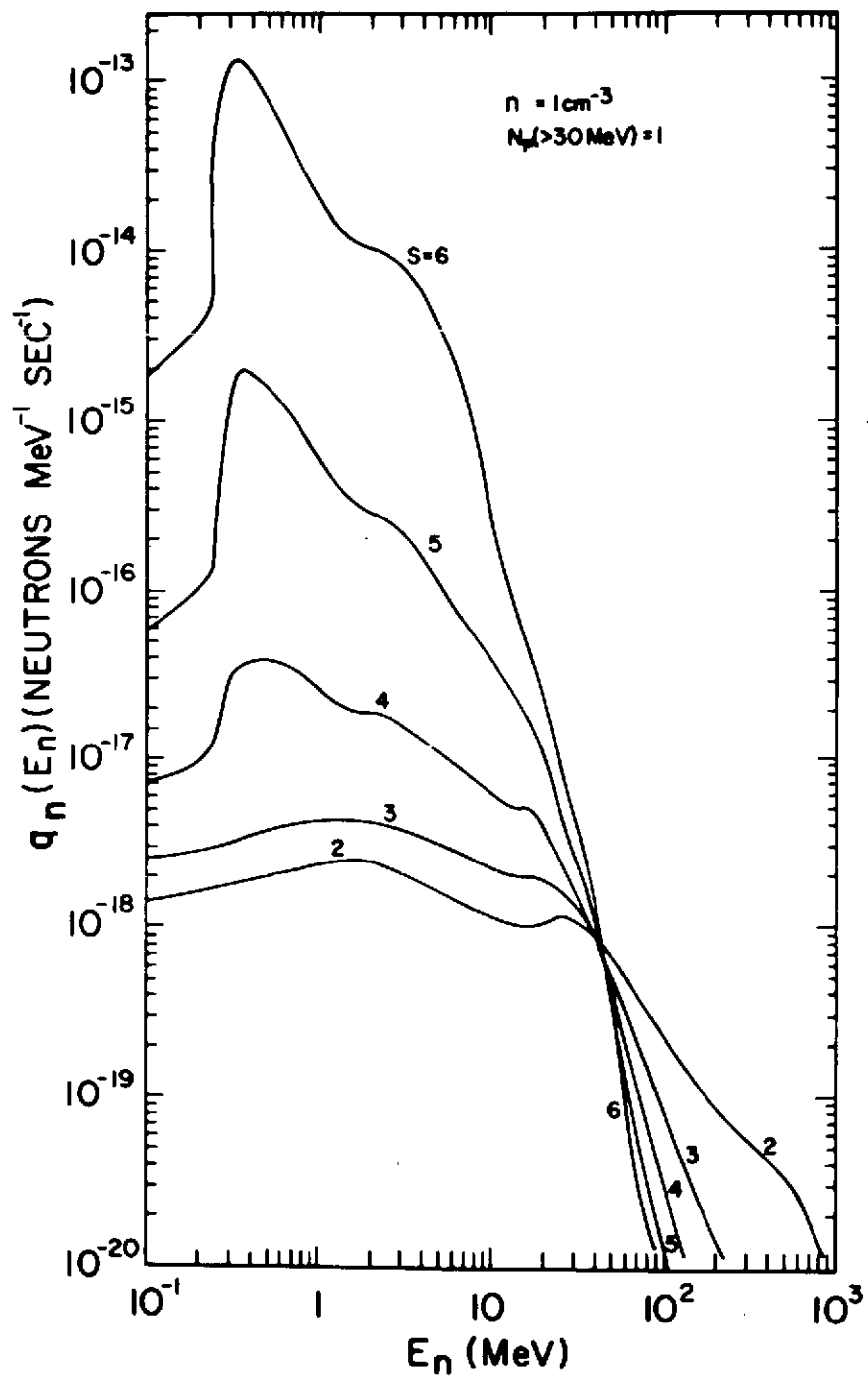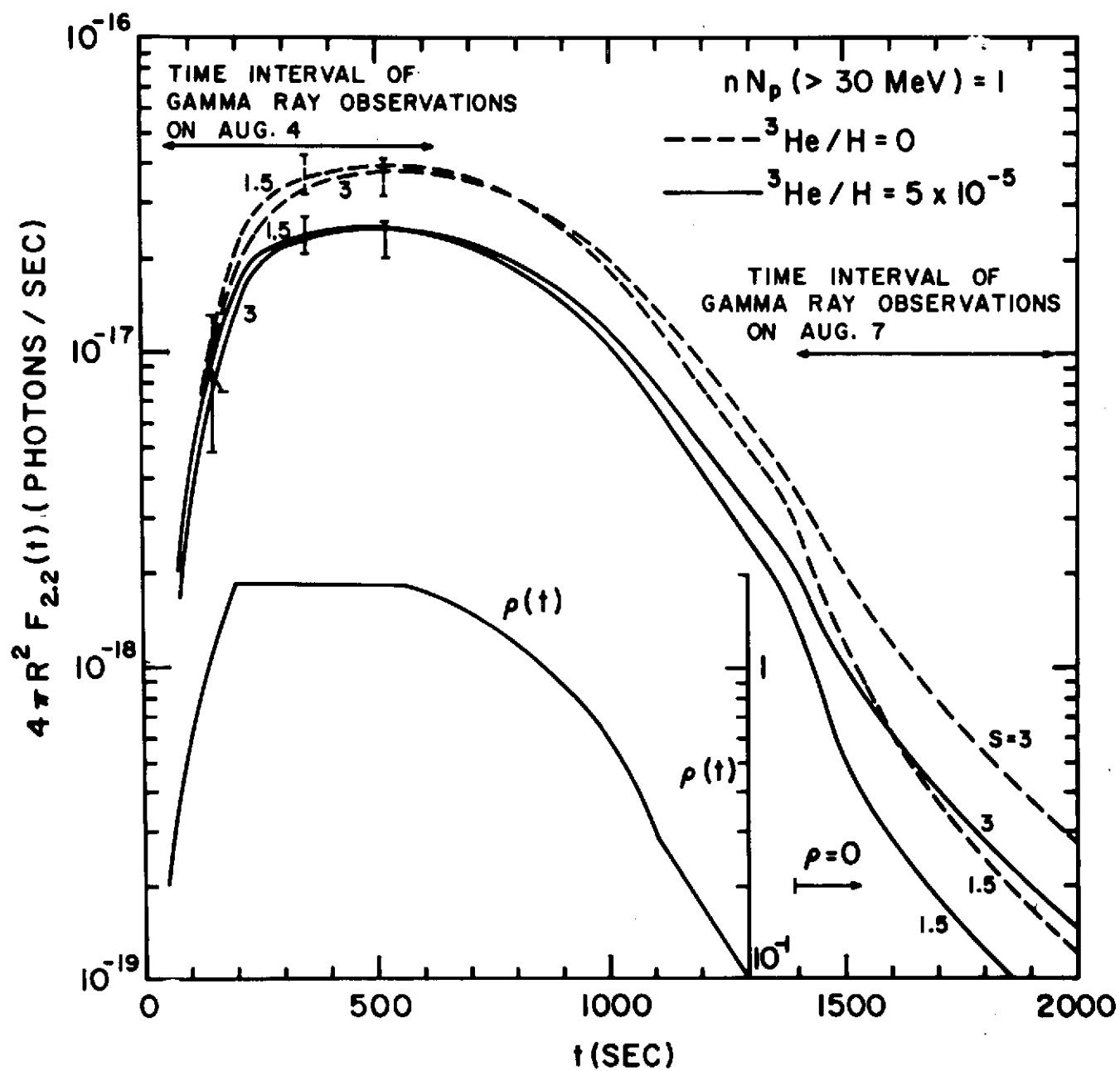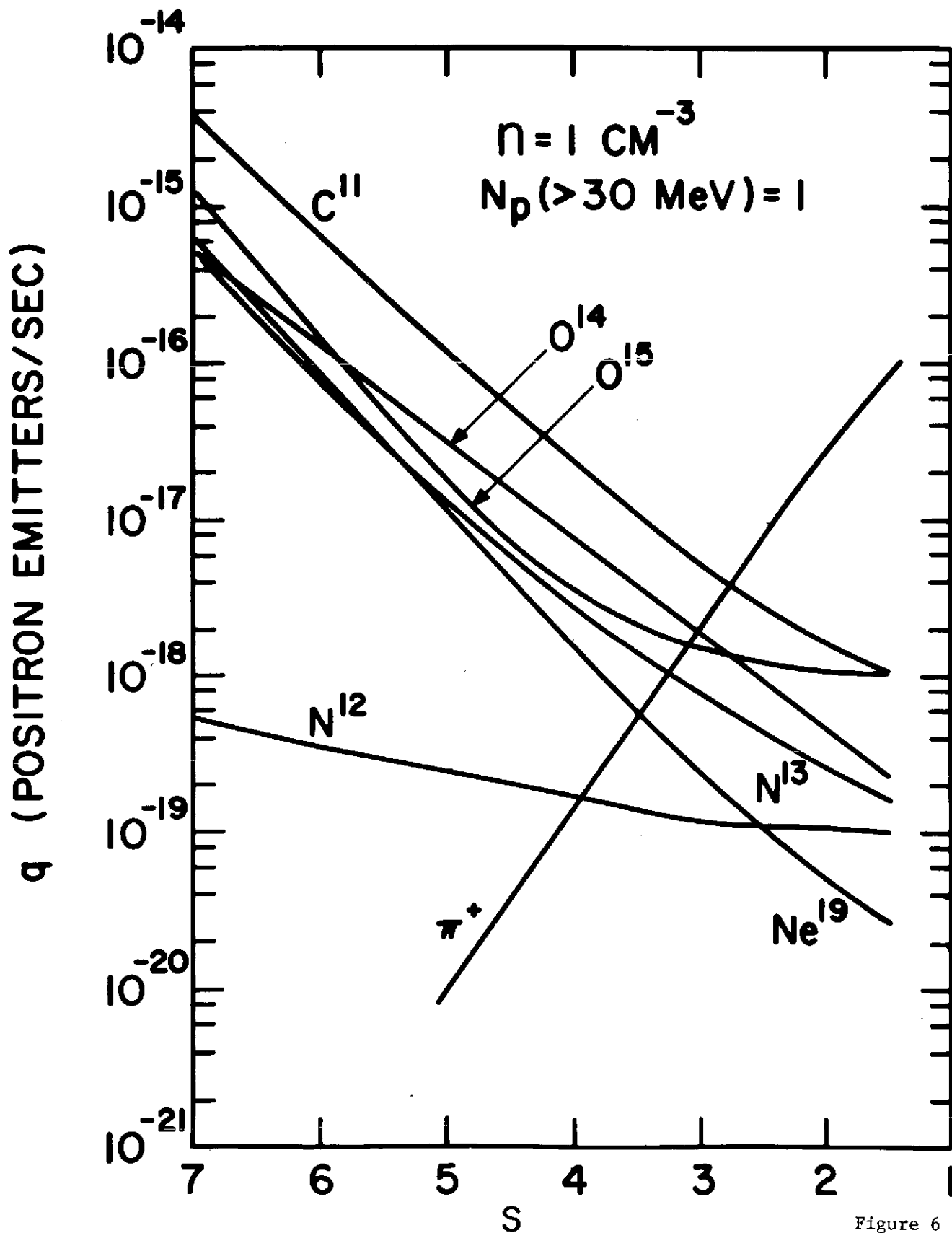15^{h}10^m 20^m 30^m 40^m 50^m

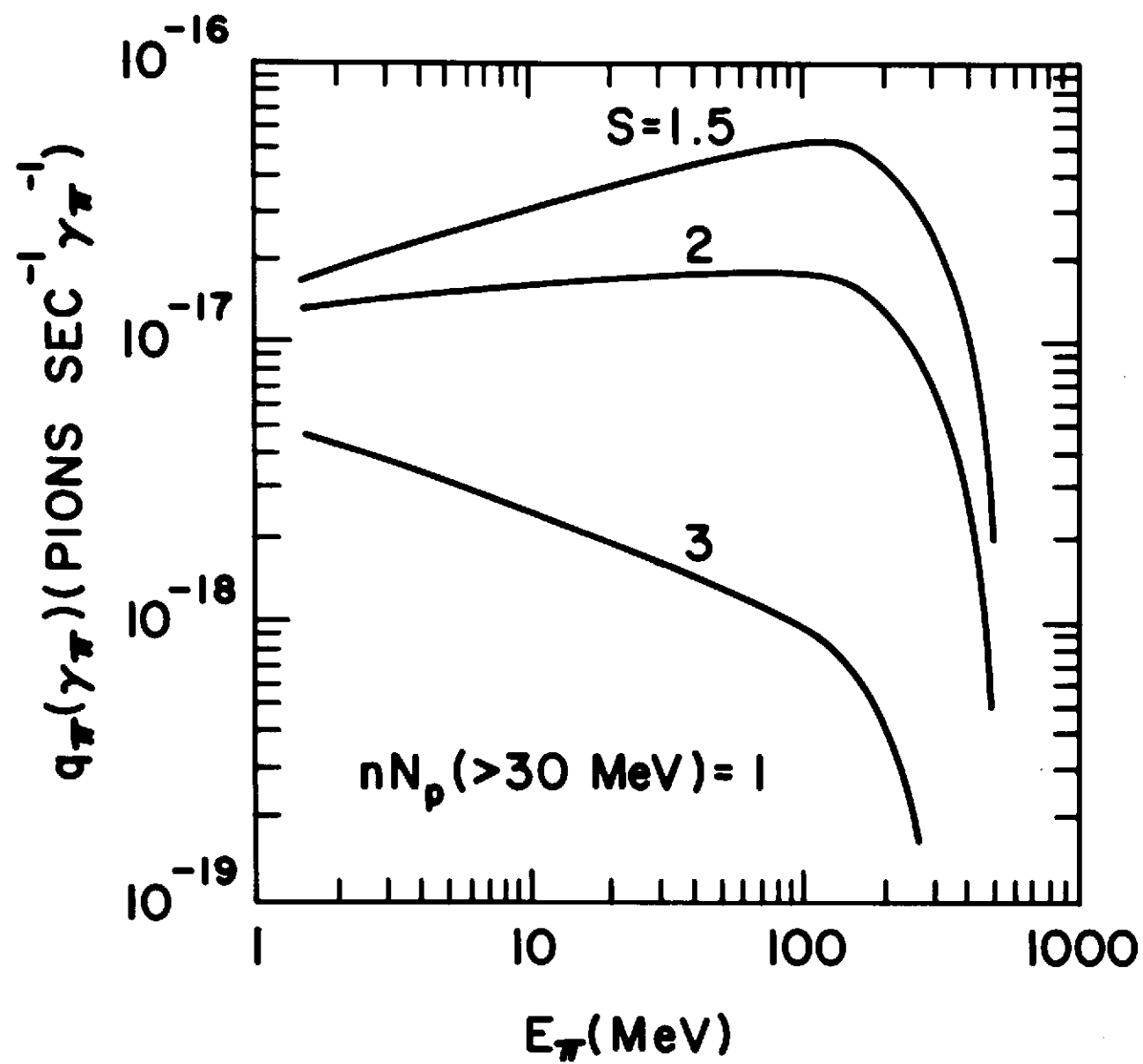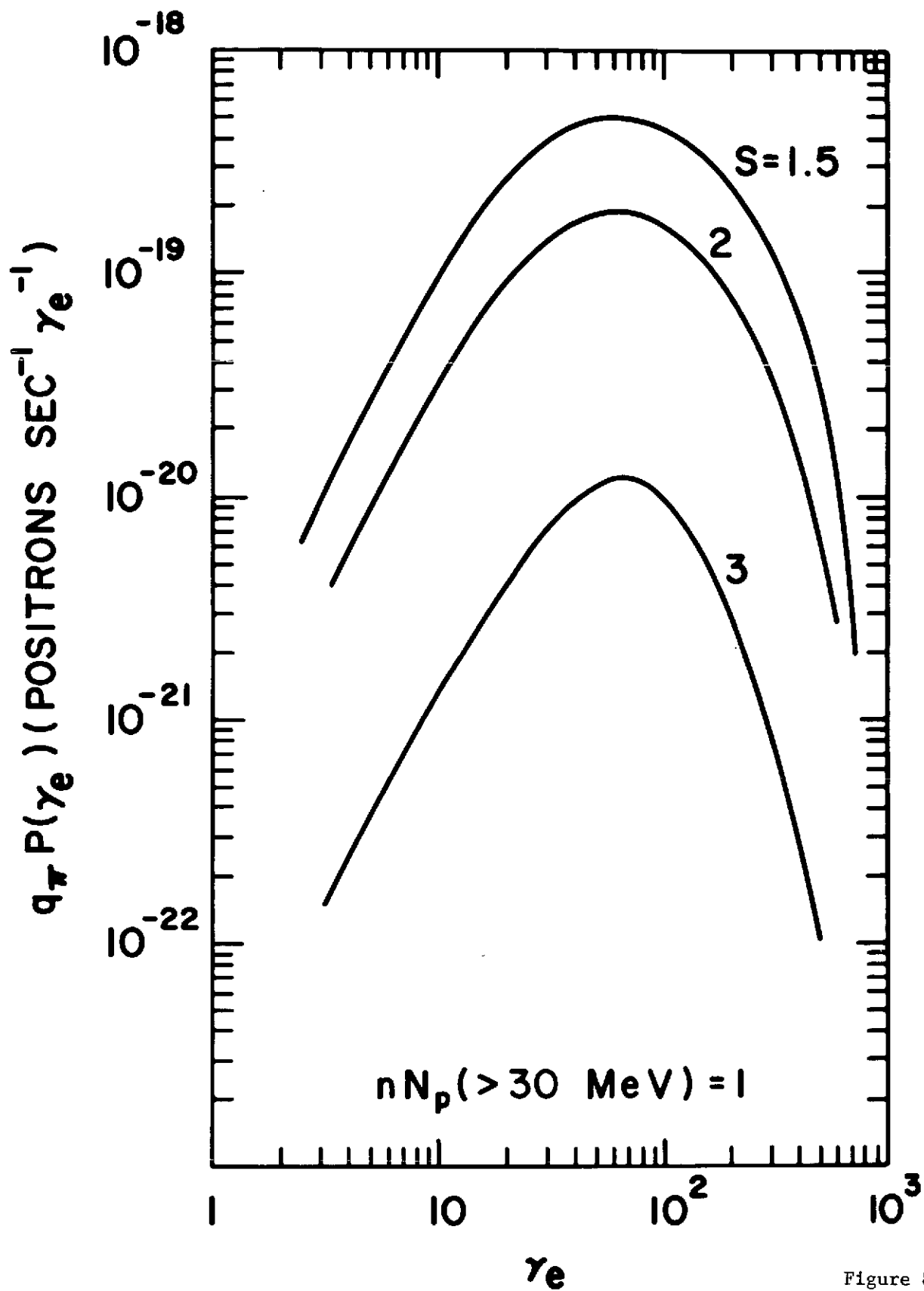GAMMA RAY
OBSERVATIONS
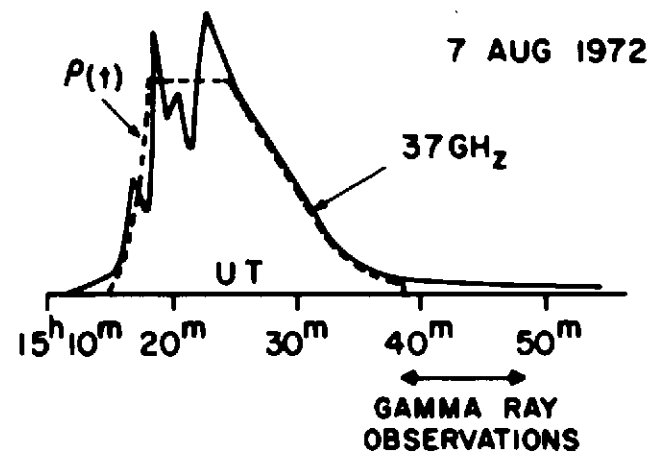
Figure 1

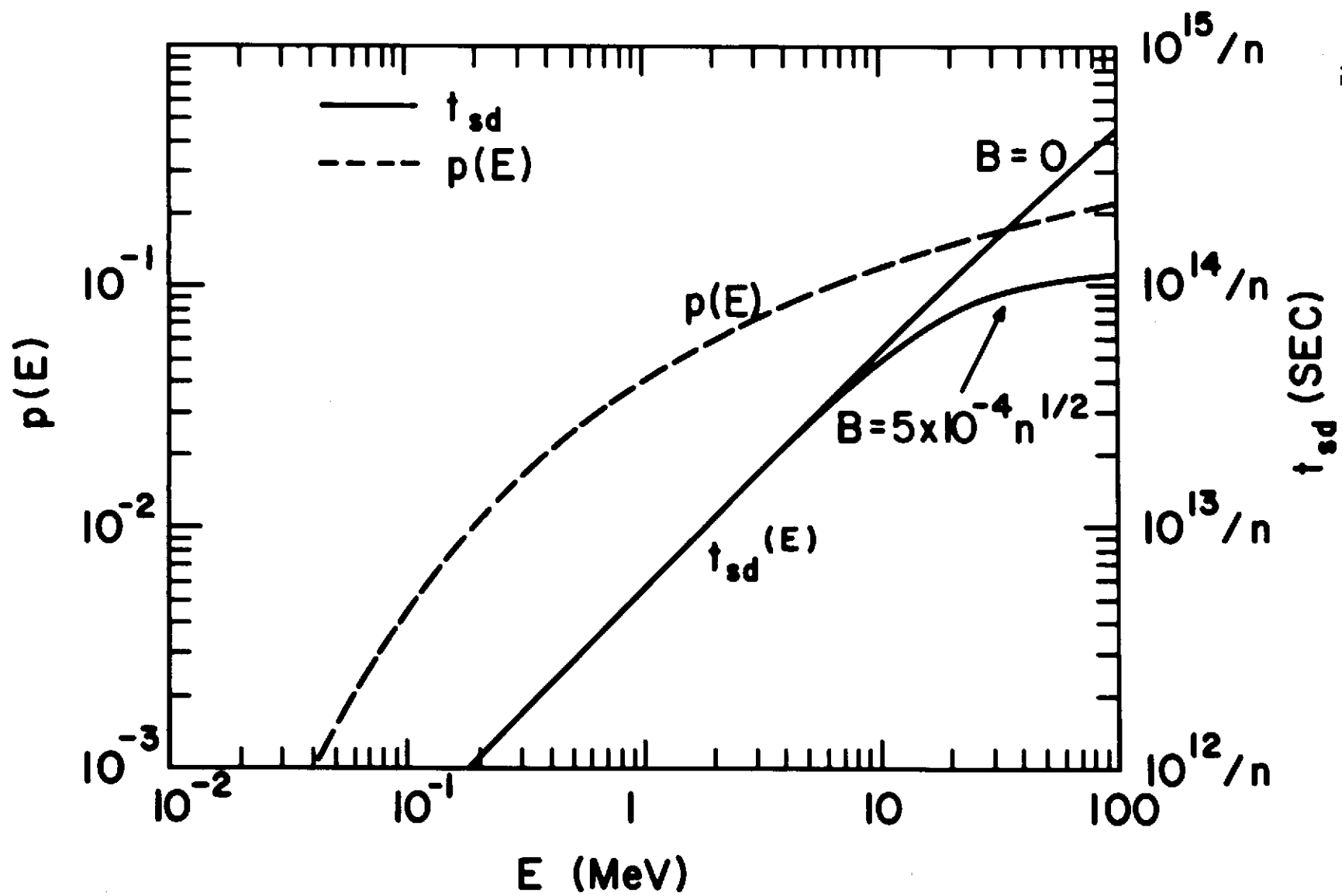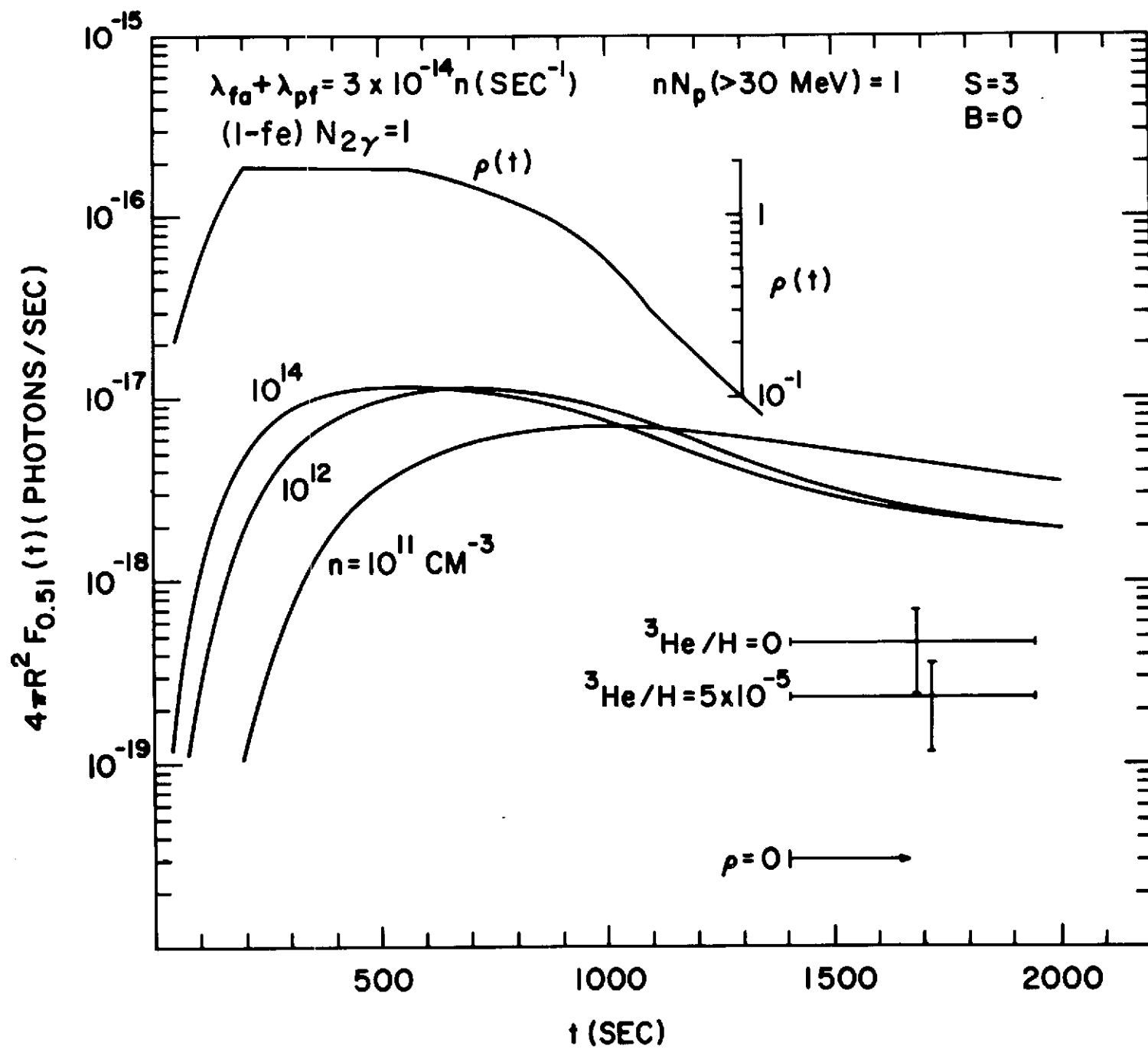Figure 2

Figure 3

Figure 4

Figure 5

Figure 6

Figure 7

Figure 8

Figure 9

Figure 10

Figure 11

Figure 12